

Signal Transmission in the Auditory System

Academic and Research Staff

Professor Dennis M. Freeman, Professor William T. Peake, Professor Thomas F. Weiss, Dr. Alexander J. Aranyosi, Dr. Bertrand Delgutte, Dr. Donald K. Eddington

Visiting Scientists and Research Affiliates

Dr. John J. Rosowski, Victor Noel, Michael E. Ravicz, Joseph Tierney

Graduate Students

Leonardo Cedolin, Andrew Copeland, Roozbeh Ghaffari, Kenneth E. Hancock, Courtney C. Lane, Kinuko Masaki, Becky Poon, Chandran V. Seshagiri, and Zachary M. Smith

Technical and Support Staff

Janice Balzer, Maggie Whearty (MEEI)

1. Middle and External

Sponsor

National Institutes of Health (through the Massachusetts Eye and Ear Infirmary)
Grants R01 DC00194, R01 DC04798

Project Staff

Professor William T. Peake, Dr. John J. Rosowski, Michael E. Ravicz

The external and middle ears are important to auditory function as they are the gateway through which sound energy reaches the inner ear. Also, middle-ear disease is the most common cause of hearing loss, and while a wide range of treatments have been developed many lead to unsatisfactory hearing results. We use measurements of middle-ear structure and function in animals, live human patients and cadaver ears in order to investigate the effects of natural and pathological variations of middle-ear structure on ear performance.

1.1 Comparative Structure and Function in Middle Ears

We have investigated the function of the external and middle ears of a highly specialized desert animal, the Sand Cat (*Felis Margarita*). The Sand Cat inhabits the Sahara and deserts of western Asia and is the only member of the cat family that lives exclusively in deserts. The Sand Cat is also unusual for its relatively large external and middle ears, structures that are much larger than those in other cats of similar body size. Our functional measurements (Figure 1) demonstrate that associated with the large Sand Cat middle ear is a large compliance of the tympanic membrane and ossicles relative to other cat species. Inclusion of the large structure of the external ear and the extreme compliance of the middle ear in a model of the auditory periphery lead to the suggestion that the Sand Cat ear is 6 to 10 dB more sensitive to sound than the domestic cat ear at frequencies less than 2 kHz (Figure 2). This increased sensitivity would lead to a significant increase in the spatial range of hearing of the Sand Cat, which may allow better identification of predators, prey and conspecifics at large distances.

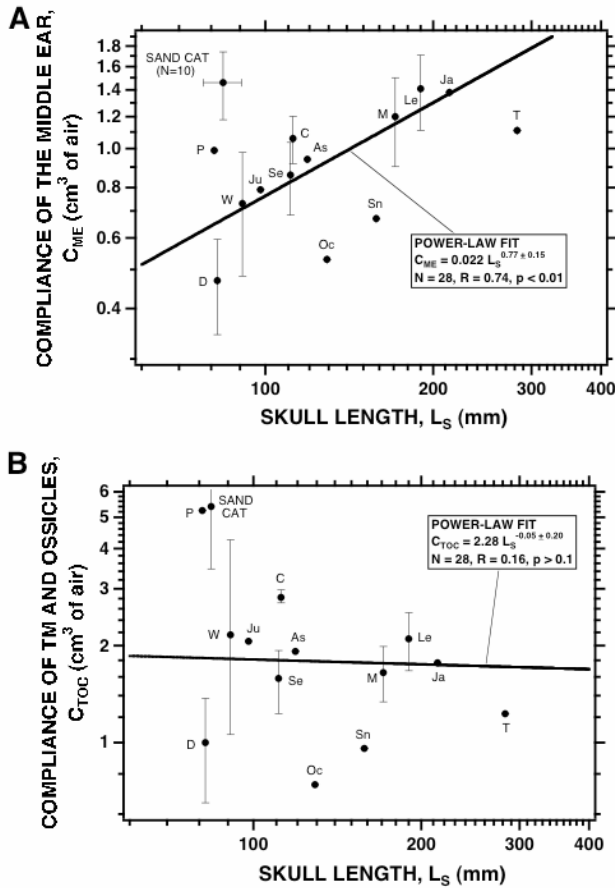


Figure 1. Plots of the variation in total middle-ear compliance and compliance of the tympanic membrane and ossicles vs. skull length (a measure of body size) in 14 cat species. The Sand Cat (in the upper left of both plots) is a clear outlier from the family trends.

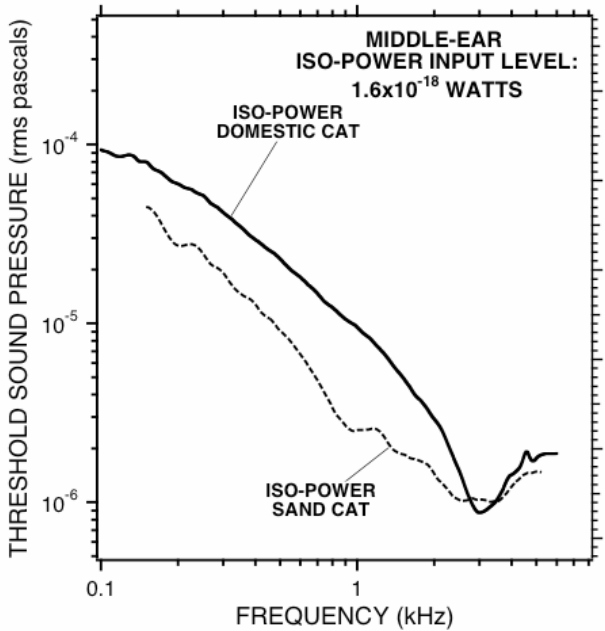


Figure 2. Predictions of auditory threshold in Sand Cat suggest a 6 to 10 dB lower auditory threshold relative to domestic cat at frequencies less than 2 kHz.

1.2 The Effect of Static Middle-Ear Pressure on the Response to Sound

Static pressure within the middle ear attenuates sound transmission, as everyone who travels in airliners knows. It had been hypothesized that one of the structural components of the tympanic membrane, the *pars flaccida* (a small flaccid section of the membrane that is not tightly coupled to the sound transmitting apparatus) plays a role in minimizing the effects of static pressure on the ear. To test this hypothesis, new mechanical measurements of the sound-induced velocity of the tympanic membrane of the gerbil were performed while varying middle-ear pressure before and after immobilizing the *pars flaccida*. The results of these measurements confirmed that static pressure has a direct influence on the mechanics of the middle ear, but also suggested that the role of the *pars flaccida* in protecting the ear from such effects was inconsequential.

1.3 The Effect of Ageing on Middle-Ear Function

It is well known that as we age the probability of middle-ear disorders increases and that our sensitivity to hearing decreases. It has been suggested that age-related changes in the middle ear are at least partially responsible for age-related changes in hearing. One complication of testing this suggestion in humans is the wide degree of variability in normal hearing function between individuals. Inbred mouse strains display much less inter-individual variability in hearing performance and also progress from new born to very old animals in a short amount of time. We made measurements of the sound-induced velocity of the tympanic membrane in young adult (6-8 weeks old), middle-aged (12 month old) and old mice (18 to 24 months old) of two different strains. The results were consistent with a small age-related reduction in middle-ear function that occurred primarily between the young adults and the middle-aged mice. However, the magnitude of these reductions (about 5-8 dB) were much smaller than the 15 to 30 dB reductions in hearing sensitivity observed in the same population. Therefore, while the data are consistent with a reduction in middle-ear function with age, the magnitude of this reduction is small compared to the hearing loss observed. We therefore conclude that age-related decreases in other aspects of auditory function, most notably inner ear function, are the more significant in age-related hearing loss.

1.4 Ossicular Pathology and Middle-Ear Response in Human Ears

We have used laser-Doppler vibrometry to measure the sound-induced velocity of the tympanic membrane in live human subjects and patients. The measurements in normal subjects have been used to determine the distribution of normal function. We also made such measurements in ears of patients with surgically determined ossicular disorders including: pathologic interruptions of the ossicular chain, bony fixations of the stapes and fixation of the malleus (Figure 3). The effect of interruption was to increase the velocity of the tympanic membrane motion, while the effects of fixation caused decreases. Both of these changes are consistent with an effect of load on the motion of the tympanic membrane. The difference in the degree of reduction observed between stapes and malleus fixation is a sign of the uncoupling of the ossicular chain by the ligaments that hold the ossicles together. Fixation of the stapes, which is separated from the tympanic membrane by two ligaments, has a smaller effect than fixation of the malleus, which is directly coupled to the tympanic membrane. The separation of the effect of the three pathologies on velocity suggests that these measurements may be useful in the pre-surgical diagnosis of ossicular disorders.

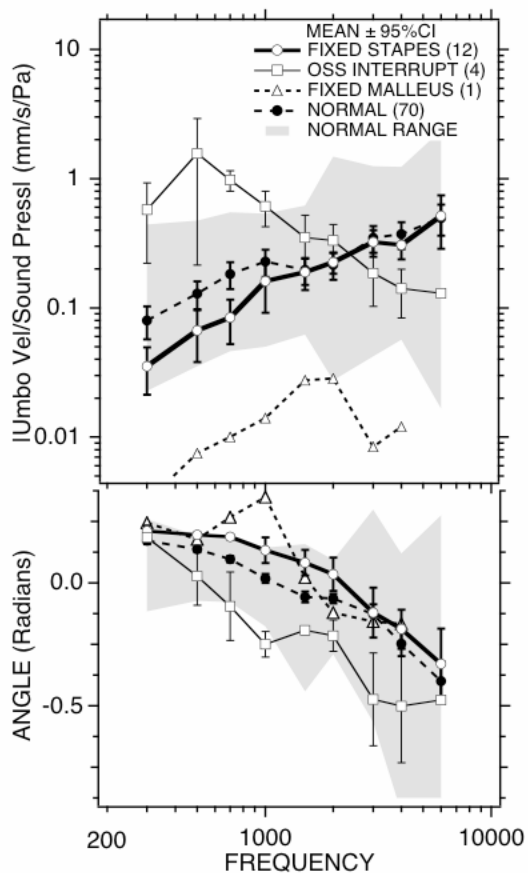


Figure 3. Comparisons of sound-induced tympanic-membrane velocity in a group on normal human subjects and three groups of human patients with pathological ears including: bony fixation of the stapes: FIXED STAPES, interruption of the ossicular chain: OSS INTERRUPT, and bony fixation of the malleus.

1.5 The Mechanics of Middle-Ear Reconstructive Surgery

We have also made measurements of the velocity of different middle-ear structures in intact, surgically modified and surgically reconstructed cadaver middle ears to investigate the functional effects of different techniques of tympanolastic surgery. These results point to a clear advantage of using an island of cartilage as part of the replacement tympanic membrane.

Publications

Journal Articles Published

G.T. Huang, J.J. Rosowski, and W.T. Peake, "Mammalian Ear Specializations in Arid Habitats: Structural and Functional Evidence from Sand Cat (*Felis Margarita*)," *J. Comp Physiol, A*, 188:663-681 (2002).

J.J. Rosowski and C.-Y. Lee, "The Effect of Immobilizing the Gerbil's *Pars Flaccida* on the Middle-Ear's Response to Static Pressure," *Hear. Res.* 174: 183-195 (2002).

Journal Articles Accepted for Publication

R.H. Mehta, M.E. Ravicz, J.J. Rosowski, and S.N. Merchant, "Middle-Ear Mechanics of Type III Tympanoplasty (Stapes Columella): I. Experimental Studies," *Otology and Neurotology*, forthcoming.

35- Communication Biophysics - Signal Transmission in the Auditory System - 35

RLE Progress Report 145

S.N. Merchant, M.J. McKenna, R.H. Mehta, M.E. Ravicz, and J.J. Rosowski, "Middle-Ear Mechanics of Type III Tympanoplasty (Stapes Columella): II. Clinical Studies," *Otology and Neurotology*, forthcoming.

J.J. Rosowski, R.H. Mehta, and S.N. Merchant, "Diagnostic Utility of Laser-Doppler Vibrometry in Conductive Hearing Loss with Normal Tympanic Membranes," *Otology and Neurotology*, forthcoming.

J.J. Rosowski, K.M. Brinsko, B.L. Tempel, and S.G. Kujawa, "The Ageing of the Middle Ear in 129S6/SvEvTac and CBA/CAJ Mice: Measurements of Umbo Velocity, Hearing Function and the Incidence of Pathology," *JARO*, forthcoming.

Books/ Chapters in Books

S.N. Merchant and J.J. Rosowski, "Auditory Physiology (Middle-Ear Mechanics)," in *Surgery of the Ear*, 5th Edition, eds. A.J. Gulya and M.E. Glasscock, III (Hamilton, Ontario, BC Decker, 2002) pg.59-82.

J.J. Rosowski and S.N. Merchant, "Acoustics for Otolaryngology," in *Basic Science for Otolaryngology*, eds. T. Van der Water and H. Staecker (Academic Press, New York) forthcoming.

Meeting Papers Published

J.J. Rosowski and C.Y. Lee, "The Influence of Static Pressure on Vibrations of the Tympanic Membrane in Animal Ears," *Abstracts of the Twenty-Fifth Annual Midwinter Research Meeting of the Association for Research in Otolaryngology*, pg 63-64, St. Petersburg Beach, Florida, January 27-31, 2002.

J.F. Holtzrichter, L.C. Ng, G.J. Burke, J.B. Kobler, and J.J. Rosowski, "EM Sensor Measurement of Glottal Structure Versus Time", *J. Acoust. Soc. Am.*, 112: 2445 (2002).

2. Cochlear Mechanics

Sponsor

National Institutes of Health Grant R01 DC00238

Project Staff

Professor Dennis M. Freeman, Professor Thomas F. Weiss, Andrew Copeland, Roozbeh Ghaffari, Kinuko Masaki

2.1. Properties of the Tectorial Membrane

Introduction

The tectorial membrane (TM) is a gelatinous structure that lies on top of the mechanically sensitive hair bundles of sensory cells in the inner ear. From its position alone, we know that the TM must play a key role in transforming sounds into the deflections of hair bundles. But the mechanisms are not clear, largely because the TM has proved to be a difficult target of study. It is 97% water, and is therefore fragile. It is small: the whole TM volume is less than that of an inch of one human hair. Finally, it is transparent.

We have developed methods to isolate the TM so that its properties can be studied. Results using this technique (which have been reported in previous RLE Progress Reports) show that the TM behaves as a gel. The material properties of a gel are a direct consequence of its molecular architecture. Charge groups on gel macromolecules attract mobile counterions from the surrounding fluid. Thus gels concentrate ions, and thereby increase osmotic pressure. The increase in osmotic pressure induces water to move into the gel and cause it to swell. The swelling stretches the macromolecules and increases the stiffness of the gel. The important consequence is that gels have mechanical, electrical, osmotic, and chemical behaviors that are all linked by their common molecular basis.

Measuring the Equilibrium Stress-Strain Relation of the TM

The important parameters of a gel are the amount of fixed charge and the elasticity of the matrix of macromolecules. A simple way to estimate the bulk modulus of a connective tissue is to place it in a dynastat, apply a hydraulic pressure, and measure the change in volume. An alternative method, one more suited to the dimensions and fragility of the TM, is to apply an osmotic pressure and measure the resultant change in volume. The simplest method to increase the osmotic pressure, without changing the ionic strength of the bath solution, is to add a non electrolyte to the bath.

Previously we have reported that polyethylene glycol (PEG), a large uncharged solute, exerts an osmotic pressure that causes the TM to shrink. However, the osmotic pressure exerted by PEG depends on molecular mass and is nonlinearly related to concentration. As a result, the osmotic pressure exerted by PEG can be more than 200 times larger than predicted by van't Hoff's law^{1,2}. Consequently, estimates of the fixed charge and matrix elasticity of the TM derived using this method are extremely sensitive to the distribution of molecular weights of PEG — a distribution that can change from batch to batch. Although we are still evaluating the effect of this nonlinearity, preliminary calculations suggest that the concentration of fixed charges in the TM is around -80 mmol/L, and the matrix elasticity is around 62 kPa. These values are significantly larger than those suggested by previous studies.

¹ V.A. Parsegian, R.P. Rand, N.L. Fuller, and D.C. Rau, "Osmotic Stress for the Direct Measurement of Intermolecular Forces," *Meth. Enzymol.*, 127: 400-416 (1988).

² H. Hasse, H.P. Kany, R. Tintinger, and G. Maurer, "Osmotic Virial Coefficients of Aqueous Poly(Ethylene Glycol) from Laser-Light Scattering and Isopiestic Measurements," *Macromolecules*, 28: 3540-3552 (1995).

Characterizing TMs from COL11A2 $-/-$ Mice

A large fraction of the protein content of the tectorial membrane consists of various types of collagen, a common protein that confers mechanical rigidity to a variety of connective tissues. Humans lacking the COL11A2 gene, which encodes for a variant of collagen type 11, have a 40-60 dB hearing loss^{3,4}. Mice that have been genetically engineered to lack this same protein (COL11A2 $-/-$ mice) have a similar hearing loss⁵. Electron microscopic images of the cochleas of these mice show that the fibrillar structure of the TM is somewhat disarrayed. We are collaborating with Dr. Richard Smith of the University of Iowa to study the mechanical properties of TMs from COL11A2 $-/-$ mice. Preliminary results show that, in contrast to their appearance in fixed tissue, the TMs of COL11A2 $-/-$ mice are roughly half the thickness of TMs from wild-type mice (Figure 1). When 10 mM PEG is added to the bath, both wild-type and COL11A2 $-/-$ TMs shrink to roughly the same size. This result suggests that deletion of the COL11A2 gene causes enormous changes in the material properties of the tectorial membrane.

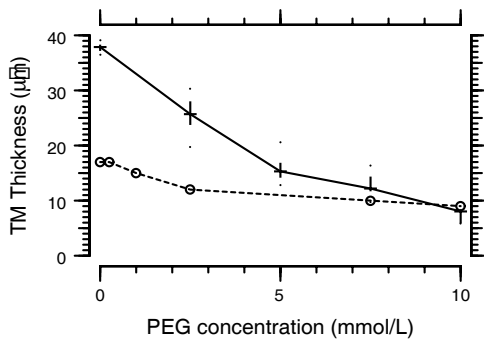


Figure 1: TM thickness as a function of PEG concentration for wild-type (solid line) and COL11A2 $-/-$ mice (dashed line). TMs from the COL11A2 $-/-$ mice were roughly half the thickness of those from wild-type mice when bathed in an artificial endolymph (PEG concentration = 0). When PEG was added to the bath, both types of TM shrank, but the wild-type shrank more. With 10 mM PEG in the bath, both types of TM were roughly the same thickness.

Microfabricated Electrodes for Probing TM Properties

Because the TM contains fixed charge, electrical measurements can provide insight into the material properties of the tissue. Electrical measurements of other connective tissues, such as cartilage, are made by placing the tissue in an Ussing chamber separating two baths, and measuring the potential between the baths. Because of its small size and fragility, the TM cannot be studied using such methods. To overcome this problem, we are developing microfabricated structures to measure electrical properties of the TM.

³ E.M. De Leenheer, H.H. Kunst, W.T. McGuirt, S.D. Prasad, M.R. Brown, P.L. Huygen, R.J. Smith, and C.W. Cremers, "Autosomal Dominant Inherited Hearing Impairment Caused by a Missense Mutation in COL11A2 (DFNA13)," *Arch. Otolaryngol. Head Neck Surg.*, 127(1): 13-17 (2001).

⁴ R.J. Ensink, P.L. Huygen, R.L. Snoeckx, G. Caethoven, G. Van Camp, and C.W. Cremers, "A Dutch Family with Progressive Autosomal Dominant Non-Syndromic Sensorineural Hearing Impairment Linked to DFNA13," *Clin. Otolaryngol.*, 26(4): 310-316 (2001).

⁵ W.T. McGuirt, S.D. Prasad, A.J. Griffith, H.P. Kunst, G.E. Green, K.B. Shpargel, C. Runge, C. Huybrechts, R.F. Mueller, E. Lynch, M.C. King, H.G. Brunner, C.W. Cremers, M. Takanosu, S.W. Li, M. Arita, R. Mayne, D.J. Prockop, G. Van Camp, R.J. Smith, "Mutations in COL11A2 Cause Non-Syndromic Hearing Loss (DFNA13)," *Nat. Genet.*, 23(4): 413-9 (1999).

One such structure is shown in Figure 2. A parallel set of electrodes is patterned onto the surface of a glass slide. The TM, which naturally adheres to the slide, is placed over the electrodes. The fixed charges in the TM attract mobile counterions, which act as charge carriers. If the TM is bathed in a non-conductive fluid, the conductance between a given pair of electrodes is related to the density of charge carriers within the TM. Simultaneous measurements of conductance and TM volume will enable us to estimate the concentration of fixed charges in the TM.

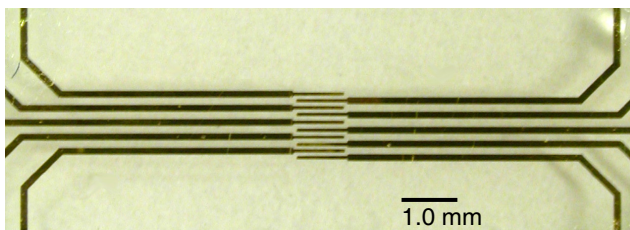


Figure 2: Experimental setup. Tectorial membranes are attached to the glass floor of a microfabricated chamber which contains ten gold electrode patterns ($0.25\ \mu\text{m}$ in depth) attached to the surface of the glass. The electrodes are driven with voltages to induce electric fields across different sections of the TM. The chamber is viewed through a microscope during experimental trials.

2.2. Sound-induced Motions of Cochlear Structures

Sponsor

National Institutes of Health Grant R01 DC00238

Project Staff

Dr. Alexander Aranyosi, Professor Dennis M. Freeman, Professor Thomas F. Weiss

Mechanical vibrations caused by sound are detected by hair cells in the cochlea. The organization of hair cells and supporting cells into a tissue determines the mechanical properties of the cochlea. To better understand the mechanics of hearing, we are studying the motions of the cochlea and its component structures in response to sound stimulation. To this end, our group has developed an in vitro preparation for studying cochlear mechanics. The cochlea of an alligator lizard is clamped in an experiment chamber so that it can be viewed with a light microscope while it is stimulated with sound. By using stroboscopic illumination and the optical sectioning property of the light microscope, we obtain slow-motion, three-dimensional images of micromechanical structures during sound stimulation. We have developed image processing algorithms to make quantitative measurements of motion directly from these images with nanometer precision.

During the past year, we have used the system to study the dynamic mechanical behavior of hair bundles, the sub-cellular structures that confer mechanical sensitivity to the cochlea. Microscopic sensory hairs extend in a hexagonal array from the surface of hair cells; hair cell receptor potentials are initiated by deflections of these sensory hairs. However, the mechanical processes that cause these deflections in response to sound stimulation are not well understood. Although computational models provide some insight — for example, in most models hair bundle deflection at high frequencies is attenuated by the fluid^{6,7,8} — existing measurements of sound-induced hair bundle

⁶ D.M. Freeman and T.F. Weiss, "Superposition of Hydrodynamic Forces on a Hair Bundle," *Hear. Res.*, 48: 1-68 (1990a-d).

⁷ D.E. Zetes and C.R. Steele, "Fluid-Structure Interaction of the Stereocilia Bundle in Relation to Mechanotransduction," *J. Acoust. Soc. Am.*, 101: 3593-3601 (1997).

⁸ L.F. Shatz, "The Effect of Hair Bundle Shape on Hair Bundle Hydrodynamics of Inner Ear Hair Cells at Low and High Frequencies," *Hear. Res.*, 141(1-2): 39-50 (2000).

deflection^{9,10} do not reveal the physical processes governing hair bundle deflection, or provide sufficient information to evaluate the predictions of current models. We have made quantitative measurements of the deflection of individual hair bundles in response to sound stimulation as a function of frequency, and used these measurements to evaluate models of hair cell function.

Hair bundle deflection was characterized by the transfer function $H_\mu(f) = \frac{\theta(f)}{U_b(f)}$, where $\theta(f)$ is the

deflection angle of the hair bundle and $U_b(f)$ is the velocity of the cochlea at the base of the bundle.

Measurements of $H_\mu(f)$ were strongly frequency dependent; the magnitude was constant or rising with frequency at low frequencies, and fell with frequency with a slope near -20 dB/decade at high frequencies. The phase was at or above 0° at low frequencies, and approached -90° at high frequencies. Consequently, at the frequencies to which the hair cells are most sensitive, the deflection of free-standing hair bundles is proportional to neither the velocity nor the displacement of the cochlea, but to some combination of the two.

The phase of $H_\mu(f)$ decreased monotonically with frequency for most hair bundles. We compared the frequency dependence of motion of different hair bundles by finding the frequency at which the phase crossed a certain value. For example, for 55 of 136 hair bundles, the phase was positive at low frequencies; that is, θ led U_b . The frequency f_T at which the phase became negative varied systematically with hair bundle height L , as shown in Figure 3. Choosing a different phase, e.g. -30°, included more hair bundles and showed a similar relation: $f_T = 1044L^{-2.13}$ ($r = -0.73$, $n = 126$). These relations are similar to the L^{-2} dependence predicted on theoretical grounds⁶.

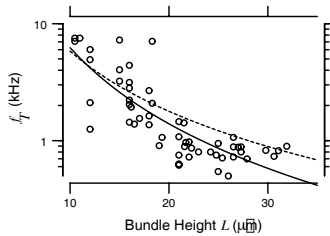


Figure 3: Relation between f_T , the frequency at which $\angle H_\mu(f)$ becomes negative, and hair bundle height L . The solid line shows the least-squares power-law fit, $f_T = 906.5L^{-2.16}$ ($r = -0.82$, $n = 55$). The dashed line shows the relation derived by Frishkopf and DeRosier⁹ from their phase measurements, $f_T = 299L^{-1.71}$.

To evaluate models of hair bundle mechanics, we have fit two models to measurements of $H_\mu(f)$ from eighty hair bundles. Measurements were normalized by the fits to facilitate comparisons of different hair bundles. The frequencies were normalized by the peak (or cutoff) frequency of each fit, and the magnitudes were normalized by the peak magnitude of the fit. The resulting normalized measurements and model predictions are shown in Figure 4. The top plots show $H_\mu(f)$ measurements normalized by the fits of a hydrodynamic flap model⁶. In this two-dimensional model, the hair bundle is represented as a flap attached by a compliant hinge to an infinite plate immersed in water. The adjustable parameters are the height L of the flap and the compliance C_z of the hinge. The measurements lie on top of the model prediction at mid and high frequencies, but the magnitudes are larger than predicted at low frequencies.

⁹ L.S. Frishkopf and D.J. DeRosier, "Mechanical Tuning of Free-Standing Stereociliary Bundles and Frequency Analysis in the Alligator Lizard Cochlea," *Hear. Res.*, 12: 393-404 (1983).

¹⁰ T. Holton and A.J. Hudspeth, "A Micromechanical Contribution to Cochlear Tuning and Tonotopic Organization," *Science*, 222: 508-510 (1983).

The bottom plots show $H_\mu(f)$ measurements normalized by the fits of a low-pass filter model. In this model the hair bundle acts as a velocity sensor at low frequencies and as a displacement sensor at high frequencies. The adjustable parameters are the low-frequency gain A and the cutoff frequency f_c . This model fits the measurements well at mid and high frequencies, but the measured magnitude and phase both diverge from the model prediction at low frequencies. In particular, the phase of $H_\mu(f)$ is often positive at low frequencies.

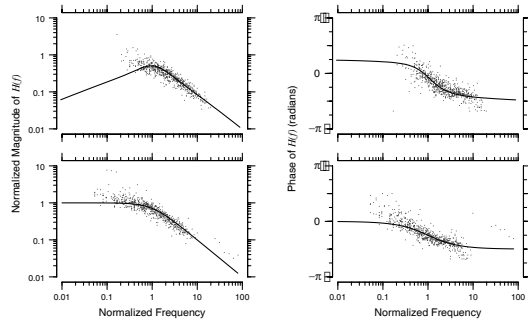


Figure 4: Normalized $H_n(f)$ values vs. normalized frequency. The top plots show the magnitude and phase of $H_n(f)$ normalized by the fits of the flap model. Dots represent individual measurements, solid lines show model predictions. The bottom plots show $H_n(f)$ normalized by the fit of a first-order low-pass filter to the data. Because the fitting and normalization were done separately for each model, the distribution of data differs in the two sets of plots.

These results show that free-standing hair bundles are neither velocity nor displacement sensors. Near the characteristic frequency of the hair bundle (normalized frequency of one in Figure 4), the slope of the magnitude response is shallower than -20 dB/decade, and the phase is between 0° and -90° . At high frequencies the magnitude of $H_\mu(f)$ falls by about 20 dB/decade, as expected of a displacement sensor, but even for frequencies ten times larger than the characteristic frequency the phase has not reached -90° . Similarly, although the magnitude may be roughly constant at low frequencies, the phase is non-zero, and is not constant with frequency. These results demonstrate the importance of solid/fluid interaction to cochlear function.

Meeting Papers Published

A.J. Aranyosi and D.M. Freeman, "Measured and Modeled Motion of Free-Standing Hair Bundles in Response to Sound Stimulation," *Biophysics of the Cochlea: From Molecule to Model*, Tony Gummer, Ed., Titisee, Germany, in press.

A.J. Aranyosi and D.M. Freeman, "A Two-Mode Model of Motion of the Alligator Lizard Basilar Papilla," *Abstracts of the Twenty-Fifth Annual Midwinter Research Meeting of the Association for Research in Otolaryngology*, p. 239, St. Petersburg Beach, Florida, January 27-31, 2002.

K. Masaki, A.D. Copeland, E.M. Johnson, R.J. Smith, and D.M. Freeman, "Measuring the Equilibrium Stress/Strain Relationship of the Isolated Tectorial Membrane," *Abstracts of the Twenty-Fifth Annual Midwinter Research Meeting of the Association for Research in Otolaryngology*, p. 240, St. Petersburg Beach, Florida, January 27-31, 2002.

Theses

A. Englehart, *Changes in a Gel's Electrical Properties Due to Exposure to Air*, S.M. Thesis, Department of Electrical Engineering and Computer Science, MIT, February 2002.

A.J. Aranyosi, *Measuring Sound-Induced Motions of the Alligator Lizard Cochlea*, Ph.D. Thesis, Harvard-MIT Division of Health Sciences and Technology, MIT, June 2002.

3. Neural Mechanisms for Auditory Perception

Sponsor

National Institutes of Health - National Institute on Deafness and Communication Disorders
Grants DC02258, DC05775, DC00119, and DC00038

Project Staff

Bertrand Delgutte, Leonardo Cedolin, Kenneth E. Hancock, Courtney C. Lane, Chandran V. Seshagiri, and Zachary M. Smith

The long-term goal of our research is to understand the neural mechanisms that mediate the ability of normal-hearing people to process speech and other significant sounds in the presence of competing sounds and how these mechanisms are degraded in the hearing-impaired. In the past year, we made progress in a number of research areas including the neural representation of pitch, neural mechanisms for binaural hearing, and physiological studies aimed at improving stimulation strategies for cochlear implants.

3.1 Neural Representations of Pitch

While pitch percepts can be produced by complex tones consisting of either resolved or unresolved harmonics, pitches based on resolved harmonics are more salient, and less dependent on phase relationships among the partials. Previous neurophysiological studies have documented a robust representation of pitch in the interspike intervals of auditory-nerve (AN) fibers and some cell types in the cochlear nucleus. These studies typically used stimuli with fundamental frequencies (F0) in the range of human voice. Because cochlear frequency selectivity is considerably poorer in most experimental animals than in humans, these stimuli contained few, if any, resolved harmonics *for the species studied*. We therefore investigated the representation of pitch in the AN for a much wider range of F0 (110-3520 Hz) than in previous studies. We find that resolved harmonics give rise to reliable rate-place cues to pitch for F0s above 400 Hz, while the representation of pitch in interspike intervals is robust up to 1200 Hz. These results suggest that both rate-place and interspike interval codes to pitch are viable, albeit in different F0 ranges.

Taken together, our studies of the coding of the pitch of complex tones in the AN, and earlier studies of Huggins dichotic pitch in the IC¹¹ suggest that pitch may be based on different neural codes depending on the stimulus and stage of processing in the auditory system. This multiplicity of codes suggests that, in order to improve pitch perception with hearing aids and cochlear implants, different processors may be required depending on the stimulus and the site of deficit.

3.2 Physiologically-realistic Model of the Discrimination of Interaural Time Differences (ITD)

In the conventional view of the neural coding of ITD, a grid of interaural cross-correlator neurons is organized along two independent dimensions: characteristic frequency (CF) and best interaural delay (BD). Recent physiological evidence from the guinea pig, however, indicates that BD actually varies with CF, such that the best phase (BP) distribution is nearly independent of CF¹². We have confirmed these findings in the inferior colliculus (IC) of anesthetized cats, and used these data to parameterize a population model of ITD coding. While previous models have simulated ITD acuity near the midline, our goal was to account for performance over the entire physiological range of ITDs.

The model is a grid of ITD-sensitive neural elements, with CF distributed along one axis according to its physiological distribution. The other axis represents the characteristic delay (CD), with values assigned based on the physiological distribution of either BD or BP. Each model element performs a

¹¹ B. Delgutte, et al., Section 33: Signal Transmission in the Auditory System, Part 3 – Neural Mechanisms for Auditory Perception, *Progress Report No. 144*, Research Laboratory of Electronics, MIT, 2001.

¹² D. McAlpine, D. Jiang, and A.R. Palmer, "A Neural Code for Low-Frequency Sound Localization in Mammals," *Nature Neurosci.*, 4: 396-401 (2001).

cross-correlation operation, in which the binaural inputs are filtered using identical bandpass filters, then cross-correlated after delaying the contralateral signal by the CD of the element. Cross-correlation values are converted to discharge rates using either a quadratic or a linear input-output function derived from physiological responses to broadband noise as a function of interaural correlation.

The model predicts the basic psychophysical finding that ITD acuity is best near the midline and degrades with increasing ITD. To obtain this result, it was necessary to distribute CD based on the physiological distribution of BP, not BD, and to use a quadratic input-output function rather than a linear one. The behavior of the model is consistent with the view that ITD coding is based on changes in firing rate, and that the location of the slope of the ITD curve is more important than the location of the peak. While previous studies have shown that pooling of information across neurons is not necessary to produce fine ITD acuity on the midline, our findings suggest that pooling is required to account for the deterioration of acuity away from the midline. Model performance was further tested by applying it to dichotic pitch, a perceptual illusion produced by the ITD processing mechanism. It was found that the ITD discrimination model also predicts the relative detectability of different interaural phase configurations of the Huggins dichotic pitch.

3.3 Neural Correlates of Spatial Release from Masking

Normal hearing individuals have a remarkable ability to hear out sounds of interest among competing sounds. In contrast, individuals with sensorineural hearing loss have difficulty listening in noise. The goal of this research is to study the neural mechanisms of spatial release from masking (SRM), the improvement in signal detection obtained when a signal is separated in space from a masker. Here, we focus on the role of neurons sensitive to interaural timing differences (ITD). Because ITD-sensitive neurons are thought to act as binaural cross-correlators, we hypothesized that a population of these neurons would show a correlate of SRM.

We record from single units in the anesthetized cat inferior colliculus (IC), focusing on low-frequency ITD-sensitive units. Stimulus azimuth is simulated using head-related transfer functions; the stimulus is a 40-Hz broadband chirp train in continuous broadband noise. For each unit, the signal-to-noise ratio (SNR) at threshold is measured at several signal and noise azimuths. Threshold is defined as the SNR at which the signal can be detected for 75% of the trials. The population threshold is defined as the best threshold across all the sampled neurons for each signal and masker combination. Additionally, we measure human psychophysical thresholds using similar stimuli to compare the neural population thresholds to behavioral thresholds.

After compensating for differences in cat and human head sizes, the spatial pattern of neural population thresholds matches that of human psychophysical thresholds. Both thresholds vary slowly with noise azimuth, and the worst threshold occurs when the signal and masker are co-located. The thresholds improve about 10 dB when the signal and noise are separated by 90 degrees.

To understand the individual unit responses that contribute to the population response, we used a simple model in which the ITD sensitivity of neurons and the dependence of responses on stimulus level are controlled by separate mechanisms. Specifically, a standard interaural cross-correlator model was used for ITD sensitivity, and a memoryless nonlinearity for the level dependence. This separable model successfully predicted responses to the noise alone as a function of both azimuth and level, and could also predict whether the signal is masked by being suppressed or swamped by the noise. However, this simple model was less successful in predicting responses to the signal and noise presented together. The signal and the noise often produce different rate responses even when their azimuth and levels are the same, presumably because of differences in their temporal structure. Current efforts are directed at incorporating these temporal effects into the model.

In summary, low-frequency ITD-sensitive units in the IC show a correlate of SRM, and the mechanism is consistent with a binaural cross-correlator model, modified to incorporate the effects of stimulus level and the temporal envelope of the stimulus.

3.4 Stimulus Coding in Small Ensembles of Auditory Neurons

Simultaneously recording from multiple neurons offers a chance to study neural correlations while increasing data yield, yet these techniques have rarely been applied to auditory brainstem nuclei. We use 'tetrodes', four channel electrodes with closely spaced recording sites ($<35\ \mu\text{m}$), to investigate the response properties of local, neural populations in the IC of anesthetized cats. Tetrodes acquire multi-unit activity and exploit the spatial sampling of the four recording sites to reconstruct single-unit spike trains. The joint information in the four channels increases the probability of identifying a neural event over using a single channel, thereby improving spike detection.

We extract single unit spike trains for up to four simultaneously recorded neurons from a recording location. In response to pure tones, all units within a local group exhibit similar best frequencies, but can differ in thresholds and temporal discharge patterns. These locally recorded units show no significant correlation beyond that induced by the stimulus. We plan to extend this technique to study the properties and interactions of local populations within iso-frequency laminae of the central nucleus of the IC.

3.5 Physiological Studies Aimed at Improving Stimulation Strategies for Cochlear Implants

While bilateral cochlear implantation is becoming increasingly common, little is known about binaural interactions in auditory neurons with such stimulation. To investigate this problem, we record evoked and single-unit responses in the inferior colliculus (IC) of acutely deafened, anesthetized cats to electric stimulation through intracochlear electrodes implanted bilaterally. Electrically-evoked auditory brainstem responses (EABR) to a biphasic pulse ($50\ \mu\text{s}/\text{phase}$) are measured for both binaural stimulation and monaural stimulation of each ear. The binaural interaction component (BIC) is computed by subtracting the sum of the monaural responses from the binaural response.

BIC amplitude varies systematically with both interaural time and level differences (ITD and ILD). The BIC is maximal with zero ITD and an ILD close to the interaural difference in EABR thresholds. When pulse thresholds of single IC neurons are measured in the same animals, the average interaural threshold difference also matches the ILD that maximized the BIC.

Single-unit responses in the IC to low-rate ($<80\ \text{Hz}$) trains of biphasic pulses are strongly phase-locked and are sensitive to ITD over a limited range of current levels. ITD tuning broadens with increasing level and saturates at 2-3 dB above threshold for some units. Higher-rate pulse trains typically only elicit onset responses. Responses to sinusoidally amplitude modulated pulse trains with a carrier rate of 1 kHz and modulation frequencies of 10-100 Hz are also recorded in some neurons. Most cells show sensitivity to interaural differences in modulation phase over a range of modulation frequencies. Overall, electric ITD tuning in some IC cells is as sharp as that seen in acoustic responses. However, dynamic range and maximum frequency of effective electric stimuli are limited.

These results are promising in that the ITD sensitivity of binaural neurons can be comparable to that found with acoustic stimulation. Nevertheless, the finding that such good sensitivity occurs over only very narrow dynamic ranges suggests that stimulation strategies for bilateral cochlear implants would have to be precisely adjusted to take advantage of such sensitivity. Further neurophysiological and psychophysical studies are needed to set the foundation for a rational design of robust stimulations strategies for bilateral implants.

Publications

Journal Articles Published

S. Kalluri and B. Delgutte, "Mathematical Models of Cochlear Nucleus Onset Neurons. I. Point Neuron with Many Weak Synaptic Inputs," *J. Comput. Neurosci.* 14: 71-90 (2003a).

S. Kalluri and B. Delgutte, "Mathematical Models of Cochlear Nucleus Onset Neurons. II. Model with Dynamic Spike-Blocking State," *J. Comput. Neurosci.* 14:91-110 (2003b).

R.Y. Litovsky and B. Delgutte, "Neural Correlates of the Precedence Effect in the Inferior Colliculus: Effect of Localization Cues," *J. Neurophysiol.* 87: 976-994 (2002).

Z.M. Smith, A.O. Oxenham, and B. Delgutte, "Chimaeric Sounds Reveal Dichotomies in Auditory Perception," *Nature* 416: 87-90 (2002).

Journal Articles Submitted for Publication

L.M. Litvak, Z.M. Smith, B. Delgutte, and D.K. Eddington, "Desynchronization of Electrically-Evoked Auditory-Nerve Activity by High-Frequency Pulse Trains of Long Duration," Submitted to *J. Acoust. Soc. Am.*

L.M. Litvak, B. Delgutte, and D.K. Eddington, "Improved Temporal Coding of Sinusoidal Electric Stimuli in the Auditory Nerve Using High-Frequency Desynchronizing Pulse Trains," Submitted to *J. Acoust. Soc. Am.*

L.M. Litvak, B. Delgutte, and D.K. Eddington, "Improved Neural Representation of Vowels in Electric Stimulation Using High-Frequency Desynchronizing Pulse Trains," Submitted to *J. Acoust. Soc. Am.*

Thesis

L.M. Litvak, *Towards a Better Speech Processor for Cochlear Implants: Auditory Nerve Responses to High-Rate Electric Pulse Trains*, Doctoral Dissertation, Harvard-MIT Division of Health Sciences and Technology, MIT, 2001.

Meeting Papers Published

L. Cedolin and B. Delgutte, "Frequency Selectivity of Auditory-Nerve Fibers Studied with Band-Reject Noise," *Abstracts of the Twenty-Fifth Annual Midwinter Research Meeting of the Association for Research in Otolaryngology*, p. 87, St. Petersburg Beach, Florida, January 27-31, 2002.

K.E. Hancock and B. Delgutte, "Neural Correlates of the Huggins Dichotic Pitch," *Abstracts of the Twenty-Fifth Annual Midwinter Research Meeting of the Association for Research in Otolaryngology*, p. 40, St. Petersburg Beach, Florida, January 27-31, 2002.

L. Cedolin and B. Delgutte, "Dual Representation of the Pitch of Complex Tones in the Auditory Nerve," *Abstracts of the Twenty-Sixth Annual Midwinter Research Meeting of the Association for Research in Otolaryngology*, Daytona Beach, Florida, February 2003.

K.E. Hancock and B. Delgutte, "Tuning to Interaural Time Difference in the Cat Inferior Colliculus: Dependence on Characteristic Frequency," *Abstracts of the Twenty-Sixth Annual Midwinter Research Meeting of the Association for Research in Otolaryngology*, Daytona Beach, Florida, February 2003.

35- Communication Biophysics - Signal Transmission in the Auditory System - 35
RLE Progress Report 145

C.C. Lane, B. Delgutte, and H.S. Colburn, "A Population of ITD Sensitive Units in the Cat Inferior Colliculus Shows Correlates of Spatial Release from Masking," *Abstracts of the Twenty-Sixth Annual Midwinter Research Meeting of the Association for Research in Otolaryngology*, Daytona Beach, Florida, February, 2003.

C.V. Seshagiri and B. Delgutte, "Simultaneous Single-Unit Recording from Local Populations in the Inferior Colliculus," *Abstracts of the Twenty-Sixth Annual Midwinter Research Meeting of the Association for Research in Otolaryngology*, Daytona Beach, Florida, February 2003.

Z.M. Smith and B. Delgutte, "Binaural Interactions with Bilateral Electric Stimulation of the Cochlea: Evoked Potential and Single-Unit Measures," *Abstracts of the Twenty-Sixth Annual Midwinter Research Meeting of the Association for Research in Otolaryngology*, Daytona Beach, Florida, February 2003.

4. Cochlear Implants

Sponsors

National Institutes of Health, NIDCD, N01-DC-2-1001
W.M.Keck Foundation
Advanced Bionics Corporation

Project Staff

Dr. Donald K. Eddington, Victor Noel, Joseph Tierney, Becky Poon, Maggie Whearty

Introduction

Cochlear implants are devices designed to restore a measure of hearing to the deaf by electrically stimulating the remaining auditory-nerve fibers. Typically, an external sound processor transforms the output of a microphone into six to twenty spectrally distinct analysis channels. The output of each channel is encoded and transmitted to an implanted receiver/stimulator that delivers each of the output waveforms to a separate metal contact of an electrode array implanted near auditory nerve fibers in the patient's inner ear.

Cochlear implantation has been restricted to a single ear for several reasons including: (1) implantation of a single ear leaves one ear to receive new technology, (2) implanting the worse ear conserved residual acoustic hearing in the unimplanted ear that could be used if the cochlear implant was not successful, and (3) evidence for bilateral stimulation had not demonstrated better performance than that provided by monolateral stimulation. Recently, bilateral implantation has become more common. This trend began with individuals implanted monolaterally with one of the early implants who received newer technology in their "other ear." Because basic psychophysical studies in these subjects seemed to demonstrate the potential for better performance with bilateral stimulation, a few centers began offering bilateral implantation as a choice for patients who suffer profound, bilateral hearing impairment.

Three patients, monolaterally implanted at the Massachusetts Eye and Ear Infirmary (MEEI), recently volunteered to serve as subjects in an NIH-sponsored research program being conducted by investigators at the Massachusetts Institute of Technology (MIT), the MEEI, Boston University, and the University of North Carolina. These subjects had received monolateral implants and volunteered to undergo implantation of their "other side" as part of our research program to develop sound processing strategies for bilateral cochlear implants.

Subjects

Each of the three subjects wore their first implant for at least six months before receiving their second implant. This made it possible to insure that their monolateral performance using the first implant was (1) not substantially improved when used together with a hearing aid in the unimplanted ear and (2) significantly better than their performance using a hearing aid alone in the unimplanted ear. Each subject received a second implant of the same model implanted in the first ear (Clarion CII, HiFocus cochlear implant system that consists of 16 electrode contacts with approximately 1 mm contact spacing).

35- Communication Biophysics - Signal Transmission in the Auditory System - 35

RLE Progress Report 145

Several pertinent subject characteristics are listed for the three subjects in Table I.

Table I: Bilaterally-Implanted Subjects				
Subject (ear)	Duration Deaf (years)	1 st Implantation (date)	2 nd Implantation (date)	CNC Score (% words)
C092(r)	5	6/2001	3/2002	98%
C092(l)	3			
C105(r)	10	6/2001	5/2002	38%
C105(l)	1			
C109(r)	3	8/2001	5/2002	90%
C109(l)	3			

We hope to accomplish two major goals in testing these bilaterally-implanted subjects before providing them with wearable, bilateral sound-processing strategies: (1) determine the optimum interaural electrode pairs for use with bilateral sound-processing strategies and (2) document bilateral and monolateral (electrically-experienced ear and electrically-naïve ear) performance on a battery of psychophysical, physiological and speech-reception measures as a function of time.

Because anatomical and physiological changes probably occur centrally as a consequence of deafness¹³ and also in response to the electric stimulation we deliver,¹⁴ we are faced with two problems. First, measures of bilateral interaction based on anatomical, physiological and perceptual measures may be dissociated in the naïve state prior to experience with bilateral stimulation. Second, the choice of the initial interaural electrode pairings may influence subsequent plastic changes and ultimate outcome. The results presented below summarize our first attempt at using psychophysical measures to guide selection of interaural electrodes. We hope these measures will lead to sound processing strategies that not only optimize short-term performance, but also provide a basis for the CNS adaptation that will maximize improvements of (1) speech reception in the presence of one or more spatially separated noise sources and (2) localization of sound sources.

Results

We began by exploring the relative pitch of interaural electrodes and found that the timbre of the sounds produced by stimulating a single electrode in the first-implanted ear was much different than that elicited by stimulation of an electrode in the second-implanted ear. All three subjects spontaneously observed that this difference was sufficiently large to make reliable pitch comparisons across the two ears impossible. Based on these subject observations, we decided to move (at least temporarily) from pitch to explore the extent to which the sensation produced by simultaneous stimulation of interaural electrode pairs would be fused (i.e., a single, punctate sound sensation).

The fusion experiment is conducted by selecting one electrode from each of the right and left electrode arrays. Each electrode of this interaural pair is stimulated alone (biphasic pulse train, 300 ms duration, cathode/anodic phase order, 108 μ s/phase, 200 pps) and the stimulus level adjusted to produce a criterion sensation level (typically just below the subject's most comfortable listening level. The interaural pair is then stimulated simultaneously and the subject asked to describe the sensation they experience. For electrodes that are cochleotopically far apart (e.g., right electrode 1 [R1] with left electrode 16 [L16]), the subject will likely report hearing two different sounds, one in each ear.


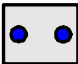

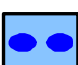



¹³ R.K. Shepherd, R. Hartmann, et al., "The Central Auditory System and Auditory Deprivation: Experience with Cochlear Implants in the Congenitally Deaf." *Acta Otolaryngol Suppl*, 532: 28-33 (1997).

¹⁴ R.L. Snyder, S. J. Rebscher, et al., "Chronic Intracochlear Electrical Stimulation in the Neonatally Deafened Cat. I: Expansion of Central Representation." *Hear Res*, 50(1-2): 7-33 (1990).

35- Communication Biophysics - Signal Transmission in the Auditory System - 35

RLE Progress Report 145

For some interaural electrode pairs that are presumably similar in cochleotopic position (e.g., L14/R13), the subject might report hearing a single, punctate (fused) sound at a location inside their head.

Table II: Fusion Experiment Responses		
Description	Fusion Score	
 Two different sounds, one at each ear	0	
 The same sound, at two different points	1	
 The same sound, at two different regions	1.5	
 Diffuse, fills head with two concentrated regions	2	
 Diffuse, fills head	3	
 Diffuse, fills head with one concentrated region	4	
 One punctate sound	5	

The range of sound sensations reported by the three subjects is large, but consistent across subjects. Table II lists the major classifications of responses we encountered in conducting the fusion experiments. The fusion scores listed in the right-hand column are a first attempt to quantify the degree of fusion associated with each class of response.

Figure 1 presents plots of the fusion data we collected for subject C092. While these data are not complete (white space represents interaural electrode pairs not tested), the results are consistent with an interpretation that interaural electrode pairs near the diagonal representing equal left/right electrode numbers are more likely to be fused.

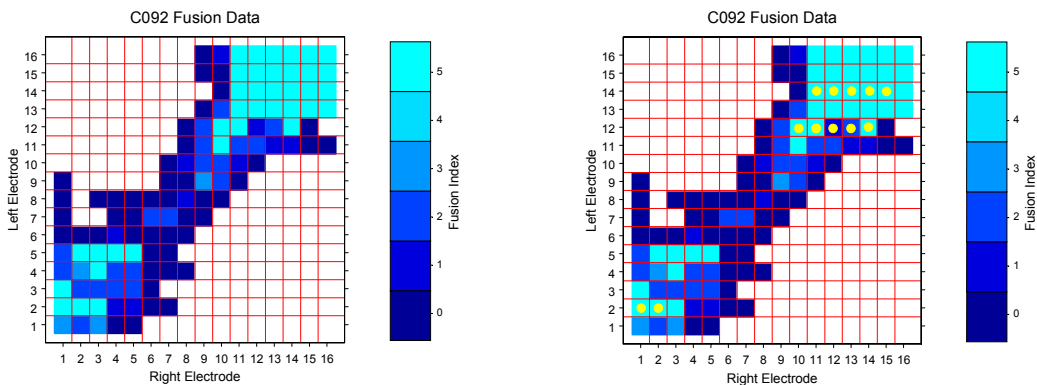


Figure 1. Plots of fusion data for bilaterally-implanted subject C092. For each interaural electrode pair tested, a color is plotted that represents the subject's response. As shown by the Fusion Scale, lighter colors represent higher Fusion Scale values (see Table II for the correspondence between the Fusion Scale and the categories of responses). White space marks interaural electrode pairs that have not been tested. In the right panel, yellow circles mark interaural electrode pairs that were tested for ITD sensitivity.

The data of C092 show a region of highly fused sensations produced by interaural electrode pairs in the upper-right quadrant. One wonders to what extent this fusion plateau indicates a large set of interaural electrode pairs with relatively good binaural sensitivity. In order to explore this issue, we measured just-noticeable differences (JNDs) of interaural time difference (ITD) for electrode pairs producing highly fused sensations in both this basal region and in the more apical region associated with L2.

Initial measures of ITD JND are shown in Figure 2 for the twelve interaural electrode pairs marked by yellow circles in the right panel of Figure 1 (see caption for a description of methods). Notice that the ITD sensitivity is far from homogeneous across these electrode pairs. In the case of right electrodes paired with left-electrode 12 (L12), the L12/R11 pair shows the highest sensitivity. When examining pairs including L14, the L14/R13 combination is most sensitive to ITD.

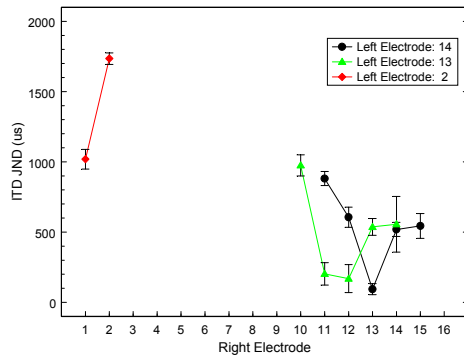


Figure 2. Plot of ITD JND as a function of interaural electrode pair. The data in black are means and standard deviations for right electrodes paired with left 14 and the green for those paired with left 13. An adaptive, two-interval, forced-choice protocol was used where the subject reported whether the sound sensation elicited by the second stimulus was to the right or left of that elicited by the first. The stimulus with ITD was randomly assigned to the first or second interval and only right-ear stimuli were delayed. Stimuli were biphasic pulse trains (300 ms, 200 pps, 108 μs /phase) with right-electrode and left-electrode levels adjusted to give a centered image with 0 ITD.

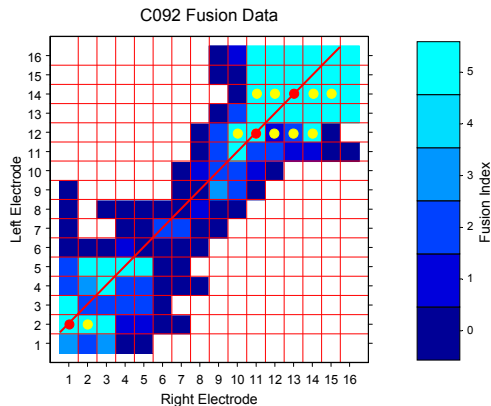


Figure 3. The circles mark the interaural electrode pairs for which ITD JND data are shown in Figure 2. For Left electrodes 14, 12, and 2, the red circles represent the pairs with minimum JND. The solid red line marks the interaural pairs used to implement a bilateral sound processor.

The interaural pair giving the best ITD-JND for L14, L12 and L2 in the data of Figure 2 are plotted as red circles on subject C092's fusion data in Figure 3. This limited set of fusion and ITD-JND results is consistent with a left electrode array that is inserted approximately 1 mm deeper in the cochlea than the right electrode array and suggests selecting a set of interaural electrodes represented by the red diagonal line for a bilateral sound-processing strategy.

Such a processing strategy has been implemented in wearable form and the subject has begun using it on a daily basis. Localization and speech reception in the presence of noise sources spatially separated from the target signals will be measured in the near future and reported in the next RLE Progress Report.